

## Chapter 2

# Online Sample Injection and Multidimensional Chromatography Separation by Using Strong-Cation Exchange Monolithic Column

### 2.1 Introduction

Nanoflow LC-MS/MS is the central platform in shotgun proteome analysis due to its high sensitivity and high separation capability. The flow rate of nanoflow LC separation is usually 50–300 nL/min. Manual injection of protein sample onto a 50–100  $\mu\text{m}$  inner diameter (i.d.) capillary LC separation column by nitrogen pressure or void capillary is feasibly achieved in previous proteome analyses [1–3]. However, this strategy is time-consuming, labor-intensive, and variations are easily introduced in the manual operations, which significantly decreases the analysis throughput and reproducibility. Automated sample injection by using a trap column with shorter column length and larger inner diameter is the most popular way in nanoflow LC-MS/MS analyses [4]. Briefly, protein samples vary from several to hundreds of microliters are loaded onto the trap column at a high flow rate in short time at first, and after equilibrium the adsorbed peptides are eluted from the trap column to a reversed phase (RP) capillary column for LC separation. There are usually two types of instrument configurations for the automated sample injection in nanoflow LC-MS/MS analyses. In the first type of configuration, the trap column and RP separation capillary column are connected by a nanoflow switching valve. The flow through from trap column is directed to waste or LC separation column during sample injection or separation by the switching valve [5–7]. Proteolytic digest without prior purification could be directly injected and cleaned up online in this case, which is important in proteome analysis due to the low sample loss. However, the void volume introduced by switching valve would seriously degrade the LC separation performance. The other one is vented column system in which trap and separation columns are directly connected via a microcross or microtee with an open/close switching valve [8–11]. A regular 6-port switching valve could be used instead of using nanoflow switching valve in this type of configuration due to the mobile phase for LC separation does not pass through the switching valve. Further, to minimize the void volume introduced by the microcross or microtee, Licklider et al. packed the open space of microcross with C18 particles to reduce void volume [8].

Meiring et al. drilled the microtee to 0.6 mm i.d. to fit a single micro sleeve having a V-shaped cut as a waste outlet, and the trap and analytical columns were butt-connected in this modified sleeve [9]. However, these systems need tedious manual operation and the reproducibility is difficult to control.

As described in Chap. 1, proteins within biological systems are extremely complex and more than 300 types of posttranslational modifications (PTMs) can be dynamically occurred. Further, the dynamic expression range of different proteins exceeds six orders of magnitude in cells and ten orders of magnitude in body fluids [12]. For large-scale protein identification, powerful separation strategies coupling to mass spectrometry are usually applied to reduce the complexity of protein analytes. And C18 RP capillary column is most widely used due to its high separation efficiency and good compatibility with ESI MS detection. To improve the LC separation performance of C18 capillary column, longer columns and/or smaller packing materials are usually utilized [7, 13, 14]. However, the operating pressure of these types of capillary columns increases dramatically, and can only be implemented using advanced LC instrumentations with ultra-high operating pressure. Multidimensional LC separation is another alternative to increase the separation capability of the whole LC system, which is typically achieved by offline or online coupling of the two columns with orthogonal retention mechanisms [15–19]. The separation capability of multidimensional LC separation depends on both of the separation performance and orthogonality of the two different dimensions and the total separation peak capacity could improve from  $\sim 10^2$  to  $\sim 10^3$  [20, 21]. Among all of these cases, C18 RP chromatography was usually utilized as the first LC dimension that directly coupled to MS, and strong-cation exchange (SCX) chromatography was most widely used as the second dimension for peptides or proteins prefractionation due to its good orthogonality to RP chromatography.

Comparing with offline strategy, online multidimensional LC separation exhibits its low sample loss and contamination, and the analysis sensitivity and throughput can be also greatly improved. Multidimensional Protein Identification Technology (MudPIT) is the most widely utilized mode of online multidimensional LC separation, and it is achieved by a biphasic capillary column packed with SCX and RP materials in sequence [1, 2, 22]. Peptides loaded onto the SCX materials are stepwise eluted to RP segment by flushing salt step, and a nanoflow RP LC-MS/MS analysis is flowed with each salt step. This online 2D LC-MS/MS is fully automated and exhibits advantages such as minimal sample loss, no vial contamination, and sample dilution. However, the LC operation pressure limits the packing amount of SCX materials, which compromise the sample loading capacity and SCX online fractionating resolution. In order to increase the sample loading amount for multidimensional separation, overloading of the SCX segment could easily occur. Further, it is time-consuming and labor-intensive to manually load protein sample onto the SCX-RP biphasic particulate column due to the relative low permeability.

Monolithic column is a good alternative to particulate column due to its extremely low back pressure, high surface area, high mass transfer rate, and high sample loading capacity [23–26]. Polymer-based organic monolithic columns with sulfonate SCX stationary phases exhibits advantages such as pH stability,

inertness to biomolecules, absence of deleterious effects from silanol, and facility for modification [23, 24]. Various strategies were developed to introduce sulfonate groups into the monolith backbone, such as adsorption of surfactants [27, 28] grafting of pore surface [29], modification of reactive monoliths [30], and copolymerization of crosslinker and monomer containing the function group [31–33]. Copolymerization of crosslinker and functional monomer is the most straightforward strategy and the sample loading capacity can be controlled by adjusting the amount of functional monomer in the polymerizing mixture [34].

As described above, the dead volume resulted from the connections between C18 trap and C18 LC separation capillary columns inevitably decreases the separation performance of the LC system, and further decreasing the dead volume is a technique challenge. Therefore, a good alternative is to develop a dead volume insensitive system for sample injection and nanoflow LC-MS/MS analysis. Instead of using C18 trap column, we found recently that SCX trap column can alleviate the influence of dead volume on LC separation in vented column system [3]. However, proteolytic digest sample must be cleaned before sample injection in order to eliminate the contamination of the LC separation column. In this chapter, the influence of void volume between trap and separation columns on the LC separation performance and proteomic coverage was systematically studied, and it was found that the influence of dead volume (varied from 0 to 5  $\mu\text{L}$ ) was nearly eliminated by using SCX trap column. Then an automatic sample injection system was constructed by using 10-port switching valve and SCX trap column, and proteolytic digest containing contaminants could be injected directly without purification. This system allowed fast sample injection at  $\sim 2 \mu\text{L}/\text{min}$ . To further improve the sample injection flow rate and the resolution in online fractionation for the SCX trap column, we then developed a phosphate monolithic capillary column by direct copolymerization of a ethylene glycol methacrylate phosphate (EGMP) and bis-acrylamide in a ternary porogenic solvent consisting dimethylsulfoxide, dodecanol and N, N'-dimethylformamide within a 150  $\mu\text{m}$ -i.d. capillary column. When coupled this phosphate monolithic SCX trap column to a C18 packed capillary column with integrated ESI tip, this system exhibited good separation performance as well as high proteomic coverage in both one- and multidimensional nanoflow LC-MS/MS analysis. Due to the extremely low backpressure of phosphate monolithic column, automated sample injection at high flow rate of 40  $\mu\text{L}/\text{min}$  could be easily achieved. This type of phosphate monolithic column provided a reliable alternative to the particulate SCX columns for proteome analysis.

## 2.2 Experimental Results

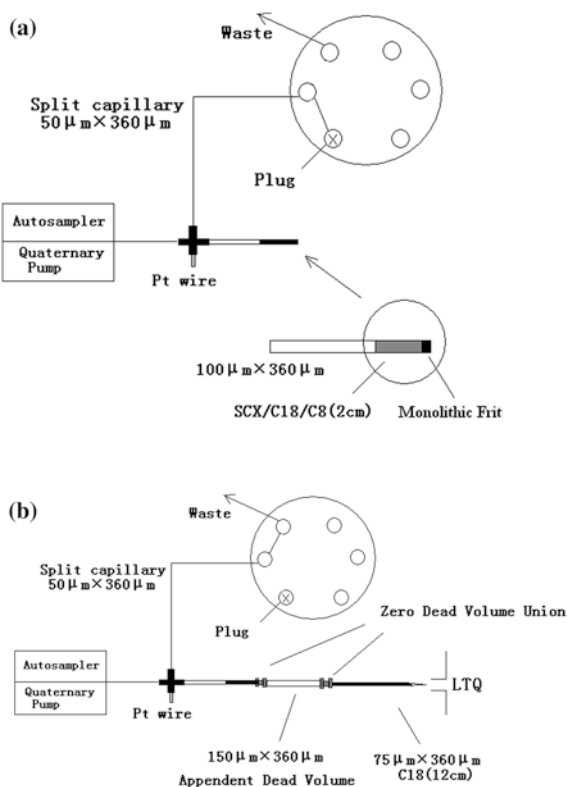
Capillary LC columns with 50–300 nL/min separation flow rate are widely applied in proteome analysis to increase the MS detection sensitivity as mass spectrometer is a concentration-dependent detector. Due to the extreme complexity and high dynamic range of protein samples, high performance LC separation is essential to large-scale

proteome analyses. C18 capillary column is the most widely used one among all the LC separation columns in proteome analyses due to the RP binary gradient separation exhibits higher separation resolution than other separation modes, such as strong-cation exchange (SCX), strong-anion exchange (SAX), and hydrophilic interaction liquid chromatography (HILIC). As C18 trap column with 100–300  $\mu\text{m}$  inner diameter (i.d.) is widely utilized for fast sample injection as described above, the dead volume between C18 trap and LC separation column compromises the performance of LC separation. Therefore, we try to eliminate this influence at first in this chapter.

### 2.2.1 The Influence of Dead Volume on LC Separation Performance Using Different Types of Trap Columns

We investigated the influence of dead volume in LC-MS/MS systems using C18, C8, and SCX trap columns, respectively. C18 trap column system was studied at first, and the dead volume of 0, 1, 3, and 5  $\mu\text{L}$  between trap and separation columns was investigated, respectively, by using different length of 150  $\mu\text{m}$ -i.d. void capillary (Fig. 2.1a, b). After LC-MS/MS analyses for 1  $\mu\text{g}$  tryptic digest

**Fig. 2.1** Schematic diagrams of the offline sample injection system to investigate the influence of dead volume on the LC separation performance, **a** loading sample onto trap column; **b** eluting sample onto analytical column and gradient RPLC analysis



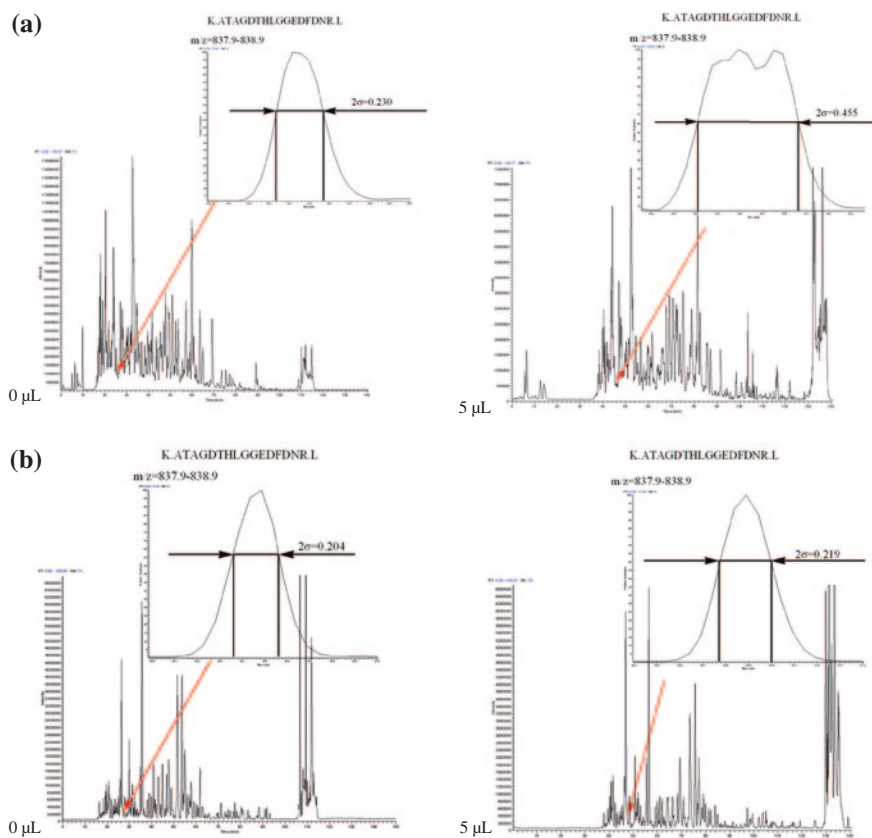


**Fig. 2.2** Base peak chromatograms for nanoflow RPLC-MS/MS analysis of 1  $\mu$ g SPE cleaned yeast protein tryptic digest on the offline sample injection system using **a** C18 and **b** SCX trap columns with void volume of 0  $\mu$ L and 5  $\mu$ L between trap and analytical columns

of extracted yeast protein, one identified peptides K.ATAGDTHLGGEDFDNR.L ( $m/z = 838$ , +2) with moderate abundance was extracted from each of the chromatogram to estimate the variation of LC separation capacity. As shown in Fig. 2.2a, the peak capacity decreased about 50 % after the dead volume increased from 0 to 5  $\mu$ L for C18 trap column system. After database searching and controlling false discovery rate (FDR) < 1 %, 544 and 382 unique peptides corresponding to 270 and 195 distinct proteins were positively identified for systems with 0 and 5  $\mu$ L dead volume, respectively. It could be seen that the peak capacity and peak intensity in LC separation, and the numbers of identified peptides and proteins were all decreased along with the increase of dead volume (Table 2.1 and Fig. 2.3a, b, the peak capacity is defined as  $n_c = L/(4\sigma)$ , where  $L$  is the total time over which the peptides eluted and  $\sigma$  is the average standard deviation of the peaks,  $2\sigma$  can be obtained as the peak width at 0.613 peak height). Obviously, the

**Table 2.1** Peak capacity and intensity for offline sample injection system by using C18, C8, and SCX trap columns with a void volume of 0, 1, 3, and 5  $\mu\text{L}$  between trap and analytical columns as well as manual injection system

Trap Column	Void volume ( $\mu\text{L}$ )	$2\sigma$	Peak capacity	Peak intensity( $10^6$ )
C18	0	0.230	200	1.82
	1	0.254	181	1.67
	3	0.290	159	1.48
	5	0.455	101	0.50
C8	0	0.242	190	0.88
	1	0.184	250	0.87
	3	*	*	*
	5	0.248	185	1.09
SCX	0	0.204	225	1.15
	1	0.208	221	1.54
	3	0.215	214	1.66
	5	0.219	210	1.03
Manual injection	\	0.189	243	2.96

\* K.ATAGDTHLGGEDFDNR.L has not been detected in this analysis

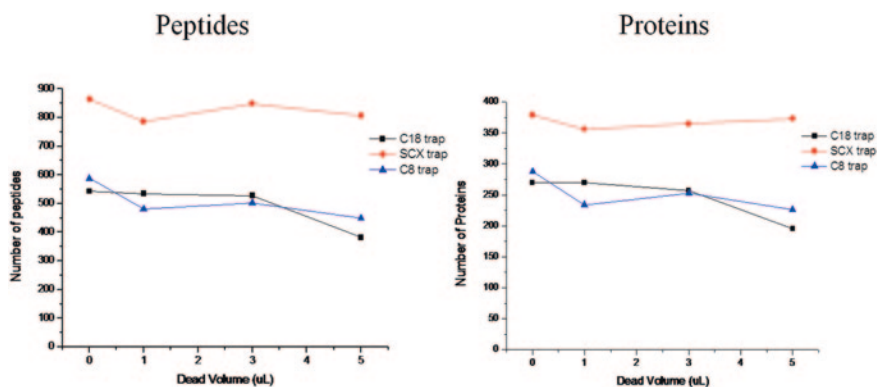


**Fig. 2.3** Effect of dead volume (between trap and LC separation columns) on the number of unique peptides and distinct proteins identified on offline sample injection system using C18, C8, and SCX trap columns (Redrawn with permission from Ref. [35]. Copyright 2007 Elsevier)

increase of dead volume between C18 trap and LC separation columns seriously decreased the LC separation capability in RP binary gradient separation, and the numbers of identified peptides and proteins both decreased  $\sim 30\%$  in proteome analysis when the dead volume increased from 0 to 5  $\mu\text{L}$ . Then, the C8 trap column was investigated in the same way as described above. Similar to C18 trap column, the numbers of identified peptides and proteins were also decreased along with the increasing of dead volume. Interestingly, the proteome coverage of C8 trap column system is inferior to C18 trap column system when the dead volume is 0  $\mu\text{L}$ , but better proteome coverage can be obtained for C8 trap column system

when the dead volume increases to 5  $\mu\text{L}$  (Fig. 2.3a, b). This can be explained by the refocusing effect of C8 trap column. As the hydrophobicity of C8 is lower than C18 materials, peptides eluted from C8 trap column will be refocused onto the head of C18 LC separation column, which can slightly alleviate the influence of dead volume on the LC separation performance as well as proteome coverage [9].

Finally, the SCX trap column was utilized and the dead volumes 0, 1, 3, and 5  $\mu\text{L}$  were also investigated, respectively. In contrast to C18 and C8 trap columns, the peak capacity and intensity in LC separation and the numbers of identified peptides and proteins were almost not changed in SCX trap column system even if the dead volume was increased from 0 to 5  $\mu\text{L}$  (Figs. 2.2b, 2.3a, b, and Table 2.1). Obviously, better performances were obtained for SCX trap column system in both LC separation and proteome coverage. A total of 379 and 373 distinct proteins were successfully identified for SCX trap column system with 0 and 5  $\mu\text{L}$  dead volumes, which increased 40 and 91 % compared with C18 trap column system at similar conditions, respectively. Similar results were also obtained for the identified unique peptides. Therefore, the numbers of identified unique peptides and proteins in the system using SCX trap column was hardly affected by the increase of dead volume (Fig. 2.3a, b). That might be explained by the migration behavior of analytes in this system. In the system using SCX trap column, the analytes migration behavior was different from C18 and C8 trap column systems. After sample was injected onto the SCX trap column, the peptides bounded on SCX resin with electrostatic interaction were eluted onto the C18 separation column by flushing with 500 mM  $\text{NH}_4\text{Ac}$  buffer (pH 3) for 10 min. Although dilution and mixing would occur in the void space when the peptides were eluted, all the peptides were re-enriched again on the front of C18 analytical column by hydrophobic interaction. When the binary gradient started for RP separation, there were no peptides eluted from SCX trap column to participate in LC separation. And the separation of peptides was only performed on the C18 separation column. Though gradient delay due to the dead volume would happen, dilution and mixing of the gradient profile would less affect the LC separation performance on C18 column (Fig. 2.2). However, in the systems using C18 and C8 trap columns, the RP binary gradient separation is started from the C18 or C8 trap column, the eluted analytes from the trap column as well as the RP gradient profile are seriously mixed and diluted within the dead volume of connecting void capillary, microtee, microcross, and union, which seriously decreases the performance of both LC separation and proteome identification (Fig. 2.3 and Table 2.1). In conclusion, the tolerance to dead volume between trap and separation columns is  $\text{SCX} \gg \text{C8} > \text{C18}$ , and SCX trap column exhibits superior performance in both LC separation and proteome analyses.

Manual injecting of protein sample directly onto the LC C18 separation column by using a void capillary can eliminate the dead volume as no trap column is needed. Thus, we also utilized manual injection of 1  $\mu\text{g}$  yeast protein digest for comparison. After nanoflow LC-MS/MS analysis, the moderated intensity peptide of K.ATAGDTHLGGEDFDNR.L ( $m/z = 838$ , +2) was also extracted from the chromatogram, and the peak capacity and intensity were 243 and  $2.96 \times 10^6$ , respectively, which is better than all of the vented systems using trap columns (Table 2.1). After database searching, 929 unique peptides from 392 distinct proteins were identified,



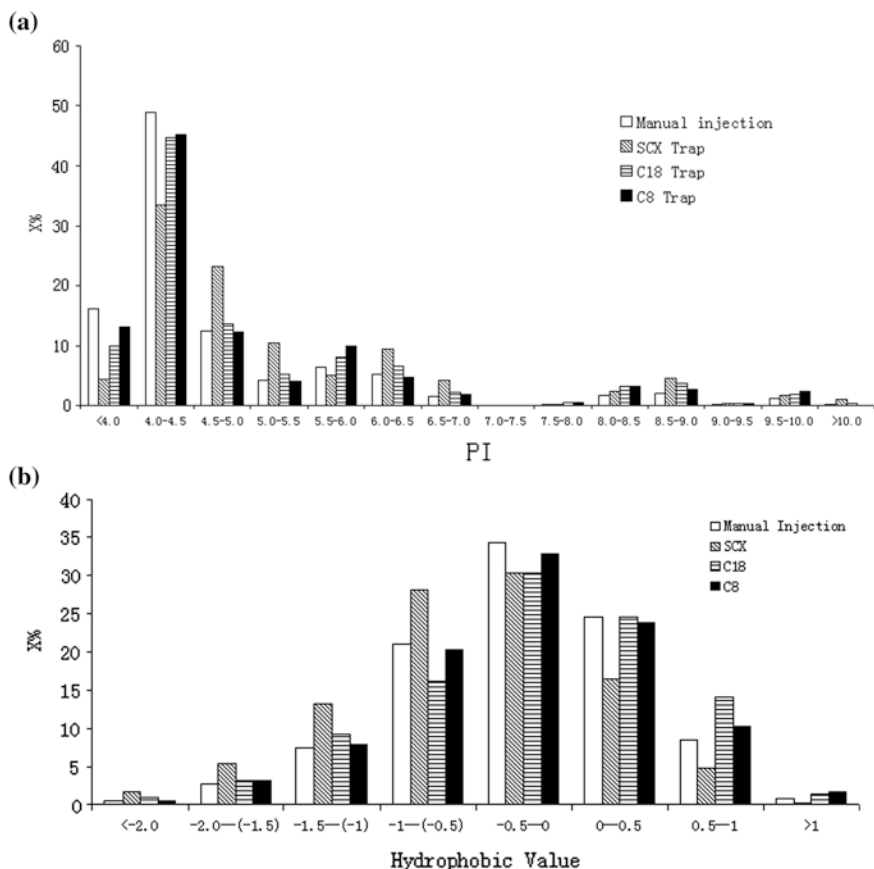


**Fig. 2.4** Distributions of **a** pI value and **b** hydrophobicity (GRAVY) for the identified peptides by nanoflow LC-MS/MS analyses in manual injection, offline sample injection by using C18, C8, and SCX trap columns with void volume of 5  $\mu$ L between trap and analytical columns (Redrawn with permission from Ref. [35]. Copyright 2007 Elsevier)

which is also better than all of the trap column systems (Fig. 2.3a, b). Therefore, the performance of both the LC separation and proteome analysis can be increased if no trap column was applied. However, manual injection is tedious and time-consuming, which decrease the throughput and reproducibility of proteome analyses. Among all of the trap columns, SCX trap column exhibits the best performance, and the numbers of identified proteins and peptides are also comparable to manual injection. Then, the pI value and hydrophobicity of all the identified peptides by different sample injection methods were calculated. It could be seen that the C18 and C8 trap columns systems could identify more peptides in low pI value range (these peptides is difficult to be charged in 0.1 % formic acid (FA) separation buffer) (Fig. 2.4a), and SCX trap column can identify more peptides in low hydrophobicity (Fig. 2.4b), which are consistent with the retention mechanism of different trap columns.



### 2.2.2 Online Sample Injection of Uncleaned Protein Sample SCX-RP 2D LC-MS/MS Analysis by SCX Trap Column

As described above, the SCX trap column has the highest tolerance to dead volume between trap and LC separation columns. Thus, we developed an online sample injection system for automated sample injection and LC-MS/MS analysis. The SCX trap column was connected with the C18 LC separation column by microfilter, nanoflow 10-ports switching valve, and microtee (Fig. 2.5). In this system, the uncleaned protein sample can be directly injected onto the trap column and the contaminants, such as salt, detergent, etc., can be online removed by the switching valve, which is important to decrease the sample loss in purification of limited amount of sample. 1  $\mu\text{g}$  uncleaned tryptic digest of yeast protein extract was automatically injected onto the SCX column and equilibrated by 0.1 % FA aqueous solution for purification. Then, the peptides were transferred to the C18 separation column by a 10 min elution of 1,000 mM  $\text{NH}_4\text{AC}$  solution (pH 2.7) and equilibrated again by 0.1 % FA aqueous solution before nano-flow LC-MS/MS analysis. The efficient LC separation window was started from 30 min in the chromatogram (Fig. 2.6a), which implied the dead volume between the trap and separation column was about 3  $\mu\text{L}$  as the separation window in manual injection was started from 15 min and the flow rate is 200 nL/min. Further,

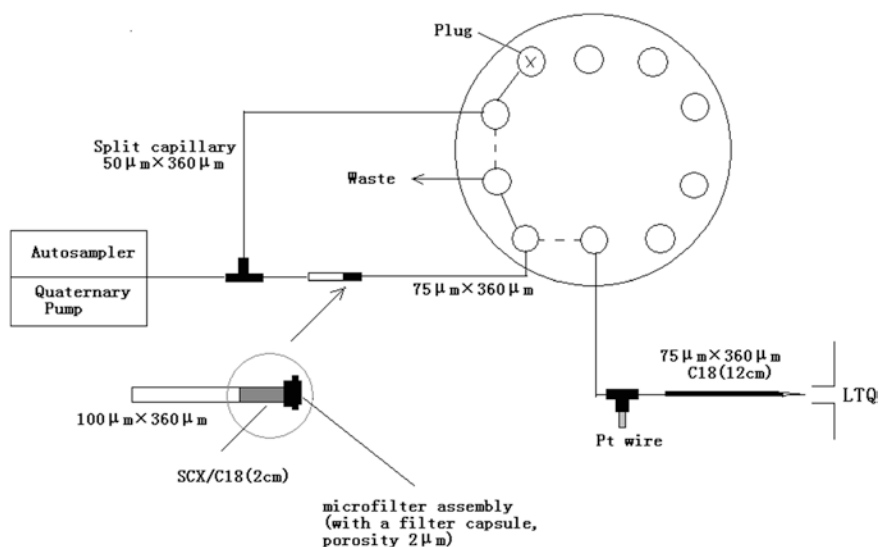


**Fig. 2.5** Schematic diagram of the system for injection of the uncleaned protein sample using 10-ports switching valve. *Solid line* loading sample onto trap column; *dashed line* eluting sample to analytical column and gradient RPLC analysis (Reprinted with permission from Ref. [35]. Copyright 2007 Elsevier)

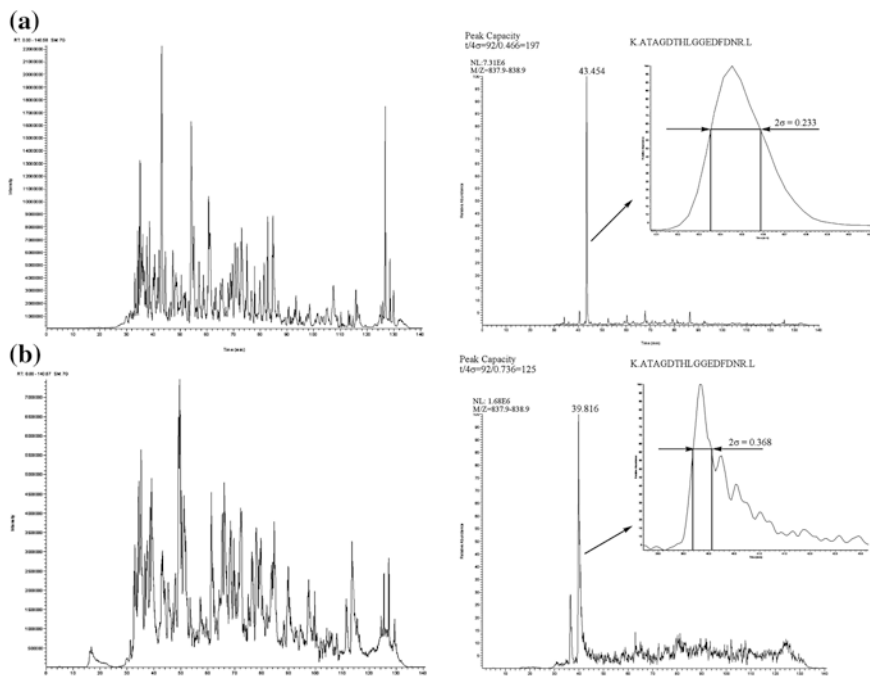


**Fig. 2.6** Base peak chromatogram for directly nanoflow LC-MS/MS analyses of 1  $\mu$ g tryptic digest of yeast proteins with online sample injection system using **a** SCX and **b** C18 trap column. The peak profile using extracted ion chromatogram corresponding to individual peptide was used for calculating peak capacity of this system (Redrawn with permission from Ref. [35]. Copyright 2007 Elsevier)

as the dead volume is consisted by microfilter, switching valve, microtee, and connecting capillary, which is much more complex than the 3  $\mu$ L dead volume introduced just by void capillary as described above in offline sample injection. Therefore, comparing to the offline sample injection system using SCX trap column, the peak width ( $2\sigma$ , at 0.613 peak height) of the moderated intensity peptide of K.ATAGDTHLGGEDFDNR.L ( $m/z = 838$ , +2) was wider in this online sample injection system (Table 2.1 and Fig. 2.6a). Finally, 1,077 unique peptides corresponding to 403 distinct proteins were identified, which were better than the results obtained by manual injection of 1  $\mu$ g SPE cleaned protein samples. Therefore, online sample cleaning by switching valve can decrease the sample loss and increase the proteome coverage, which is especially benefit for limited amount samples analyses. C18 trap column was also applied for comparison, and the detected peptide peak was seriously expanded and branched. After dataset searching, only 405 unique peptides corresponding to 195 proteins were identified. These results also demonstrated that the SCX trap column has much higher tolerance to dead volume between trap and C18 LC separation columns.

**Table 2.2** Run-to-run retention reproducibility<sup>a</sup> of four consecutive analyses of yeast protein tryptic digest by online sample injection system using SCX trap column

Mass	Retention time					RSD (%)
	Run 1	Run 2	Run 3	Run 4	Ave.	
1,424.66	29.82	30.99	33.62	31.73	31.54	4.4
2,011.02	35.72	37.14	39.57	37.82	37.56	3.7
2,294.02	42.85	44.20	46.50	45.00	44.64	3.0
3,000.40	51.38	52.22	53.92	53.14	52.66	1.8
1,427.68	57.86	59.18	61.12	60.34	59.62	2.1
2,058.02	61.66	62.89	64.84	64.13	63.38	1.9
1,815.98	66.88	67.92	70.12	69.63	68.64	1.9
1,199.67	71.88	73.24	75.15	74.44	55.37	2.5
2,418.13	78.22	79.27	81.06	80.63	79.80	1.4
1,278.66	85.36	86.95	88.96	88.26	87.38	1.6
1,719.87	91.72	93.99	95.67	94.94	94.08	1.6
2,143.13	99.58	104.18	106.03	105.12	103.73	2.4
2,577.27	102.38	106.36	108.08	107.42	106.06	2.1
2,168.18	109.53	111.70	112.61	112.09	111.48	1.1
1,821.92	122.54	124.45	124.68	124.87	124.13	0.8

<sup>a</sup>Peptides are randomly selected across the elution, sample loading rate was 2  $\mu\text{L}/\text{min}$ , and other conditions are the same as Fig. 2.6a

Reprinted with permission from Ref. [35]. Copyright 2007 Elsevier

Then, the reproducibility of this automated nanoflow LC-MS/MS system with SCX trap column was further evaluated, and four replicated analyses were performed. The retention time of 15 peptides was obtained from corresponding elution profiles in chromatograms and the relative standard deviations (RSDs) were all  $<5\%$  (Table 2.2). After database searching, the average numbers of identified unique peptides and proteins were 1,053 and 403, and the RSDs were 6.0 and 2.9 %, respectively, for four-time replication.

Although RP binary gradient separation exhibits better separation capability than other LC separation modes, the separation capability is still not enough due to the extreme complexity of protein samples as described in introduction of this chapter. Therefore, multidimensional LC separations by combing LC columns with different separation mechanisms are rapidly developed for proteome analyses in recent years. The most common combination in multidimensional LC separation is SCX and RP due to their good orthogonality. Online SCX-RP two-dimensional LC separation is applied for qualitative and quantitative proteome analyses due to its high separation performance and high detection sensitivity. In our automated sample injection system by using SCX trap column, online two-dimensional LC separation can be easily achieved by online stepwise elution of different concentration of  $\text{NH}_4\text{AC}$  buffer (pH 2.7) as described in Experimental Section. Therefore, this automated online two-dimensional LC separation system was utilized for high efficient separation of 20  $\mu\text{g}$  tryptic digest of yeast

protein extract. The digested peptides were online cleaned by the SCX trap column, followed by 13 steps online fractionations, and one nanoflow LC-MS/MS analysis was applied after each fractionation. Finally, 2,388 unique peptides and 870 proteins were successfully identified. Comparison to one-dimensional RP LC separation, the proteome coverage increased 120 %, and the distribution of peptides pI values and hydrophobicity was more symmetrical (data not shown). Therefore, for complex protein sample analysis, online SCX-RP two-dimensional separation can greatly improve the proteome coverage and detection sensitivity.

### ***2.2.3 The Preparation and Characterization of Phosphate SCX Monolithic Column***

In the previous works, the particulate SCX column packed with sulfonate silica gels was utilized for online sample injection and SCX-RP 2D LC-MS/MS analyses. One major disadvantage of packed SCX column is the high back pressure, which greatly limits the packed length and sample loading amount. And overloading of protein sample is easily happened in the system using packed SCX column for sample injection, which will decrease the resolution of SCX chromatography in online fractionation. Therefore, increase of the sample loading capacity of SCX trap column is essential to increase both the performance of SCX-RP online two-dimensional LC separation and the identified proteome coverage. Comparing with packed capillary column, capillary monolithic column has higher permeability and specific surface area, and has been already widely applied in capillary electrochromatography (CEC) analyses of different samples. However, the application of monolithic column in proteome analyses of complex biological samples is still limited, especially for SCX monolithic column. SCX monolithic columns, prepared by various sulfonate functional monomers, have been prepared and applied in CEC separation. However, the sulfonate SCX monolithic columns always exhibit extra swelling or shrinking during the change of different LC separation buffer, such as ACN and aqueous solutions [30–32]. Furthermore, it is observed that the conventional SCX monolithic columns always have part of RP retention mechanism besides SCX retention mechanism [34, 36]. Also this type of SCX monolithic column with mix retention modes sometimes have better separation performance for specific analytes, the orthogonality to RP separation will decrease in multidimensional LC separation. Therefore, it is important to develop new type of SCX monolithic column with pure SCX retention mechanism, high stability, and high sample loading capacity to further increase the LC separation performance of SCX-RP 2D LC system for complex protein sample analyses. In our previous work, a phosphate SCX monolithic capillary column was prepared by direct copolymerization of a EGMP and bis-acrylamide in a ternary porogenic solvent consisting dimethylsulfoxide, dodecanol and N, N'-dimethylformamide. It was demonstrated that this phosphate monolithic column was able to specifically isolate phosphopeptides after  $\text{Zr}^{4+}$  was loaded onto the column [37]. Therefore, we also

investigated if this phosphate SCX monolithic column can be used as trap column for fast sample injection and SCX-RP 2D LC separation.

In order to increase the sample loading capability as well as the sample loading rate, we synthesized the phosphate monolith in confined 150- $\mu\text{m}$ -i.d. capillary column, and the obtained monolith was characterized by scanning electron micrograph as shown in Fig. 2.7. It can be seen that the monolithic bed closely linked to the pretreated capillary wall and macropores are feasibly formed by the trinary

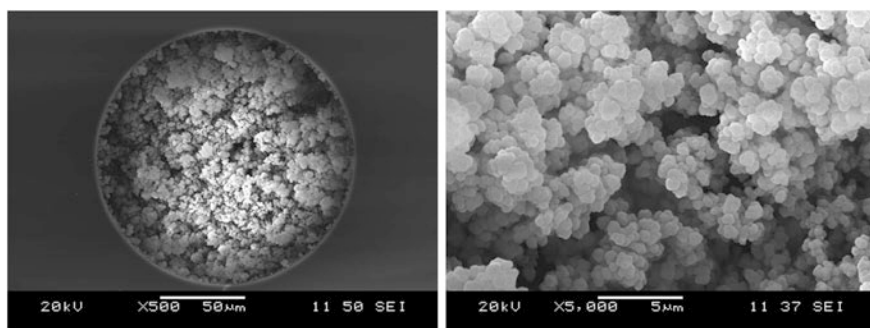


**Fig. 2.7** Scanning electron microscopy photographs of phosphate monolith inside a capillary with 150  $\mu\text{m}$ -i.d. at magnification of 500 $\times$  and 5,000 $\times$  (Reprinted with permission from Ref. [38]. Copyright 2007 American Chemical Society)

**Table 2.3** Permeability of different trap columns

Column (150 $\mu\text{m}$ i.d.)	Flushing solution	Viscosity, $\eta$ (cP) <sup>a</sup>	Back pres- sure, $\Delta P$ (psi)	Flow rate, $F$ ( $\mu\text{L}/\text{min}$ )	Permeability, $k$ ( $\times 10^{-14} \text{ m}^2$ ) <sup>b</sup>
Phosphate monolithic column (7 cm)	Acetonitrile	0.369	594.5	80	47.5
	Water	0.890	1,290.5	40	26.4
Particulate SCX column (1 cm) <sup>c</sup>	Acetonitrile	0.369	1,483.4	80	2.7
	Water	0.890	2,128.6	40	2.3
Particulate C18 column (1 cm) <sup>c</sup>	Acetonitrile	0.369	1,348.5	80	3.0
	Water	0.890	1,679.1	40	2.9

Reprinted with permission from Ref. [38]. Copyright 2007 American Chemical Society

<sup>a</sup>Viscosity data were from Ref. [34]

<sup>b</sup>Permeability can be calculated by Darcy's Law,  $k = \eta L F / (\pi r^2 \Delta P)$ , where  $\eta$  is the viscosity,  $L$  is the column length,  $F$  is the solvent flow rate,  $r$  is the radius of trap column, and  $\Delta P$  is the column back pressure

<sup>c</sup>The packed length of particulate trap columns was kept at 1 cm due to the pressure limit at high flow rate

porogenic solvent. Monolithic column used in proteome analysis should be stable enough in different separation buffers and not exhibit extra swelling or shrinking, which always influences the permeability of monolith. Therefore, we investigated the permeability of the phosphate monolithic column as well as the particulate SCX and C18 columns packed with 5  $\mu\text{m}$  diameter materials under the solutions of ACN and water, and the obtained results were shown in Table 2.3.

Obviously, the permeability of phosphate monolithic column is 15 times higher than that of particles packed columns under flowing with acetonitrile containing 0.1 % FA and about 10 times higher with 0.1 % FA aqueous solution. It is reported that sulfonate monolith swells in more polar solvents and shrinks in less polar solvent, similar phenomena were also observed in our experiments [34]. However, the permeability decreased only 44 % when the flushing solution was changed from acetonitrile to water for the phosphate monolithic column and relatively low back pressure  $\sim 1,300$  psi was observed under the high flow rate of water at 40  $\mu\text{L}/\text{min}$ . Though slightly swelling in aqueous buffer and shrinking in organic buffer will occur, no detachment of the monolith from the capillary wall was observed at any conditions applied in our experiments. The phosphate monolith was stable enough for continuous usage of 3–4 weeks with a constant back pressure.

As described above, sample loading capacity is one of the most important properties of an ion-exchange chromatography column, which determines the resolution, column capacity, and gradient elution strength. Therefore, a synthetic peptide Leu-Trp-Met-Arg-Phe- $\text{NH}_2$ . $\text{HCOOH}$  (Mw: 798.42), which bears a +2 charge at pH 2–3, was used to determine the dynamic binding capacity of phosphate SCX monolithic column (150  $\mu\text{m}$  i.d., 7 cm). A sharp increase in the baseline could be observed when the column was saturated (Fig. 2.8). After the phosphate monolithic column was saturated with the peptides, the binding peptides were flushed with 120  $\mu\text{L}$  1,000 mM  $\text{NH}_4\text{AC}$  buffer by syringe manually. Then, it was reconnected into the system and the capacity was measured again. The binding capacity was measured three times for each of the trap column. Void time estimated by flushing benzoic acid in the same column was subtracted from the total time consumed for saturating. And finally, the average time for saturation was 17.29 min in three measurements (RSD, 1.6 %) for the phosphate monolithic column. As the flow rate was 20  $\mu\text{L}/\text{min}$ , the dynamic binding capacity of the phosphate monolithic column was 140 mg/mL, corresponding to 175  $\mu\text{equiv}/\text{mL}$ . Binding capacity of particulate SCX column with 150  $\mu\text{m}$  i.d.  $\times$  2 cm was also measured following the same procedures. The average time for saturating the particulate SCX column was 4.41 min in three times measurements (RSD, 13.6 %), and the dynamic binding capacity was 125 mg/mL, corresponding to 156  $\mu\text{equiv}/\text{mL}$ . However, the packed length of the particulate column was not further increased due to the limitation of the system pressure.

Therefore, the phosphate monolith in unit volume has larger sample loading capacity than the Polysulfoethyl A. Figure 2.8 shows the frontal analysis curves of the synthetic peptide on the SCX monolithic and particulate columns. The frontal analysis curve of phosphate monolithic column increases more sharply,

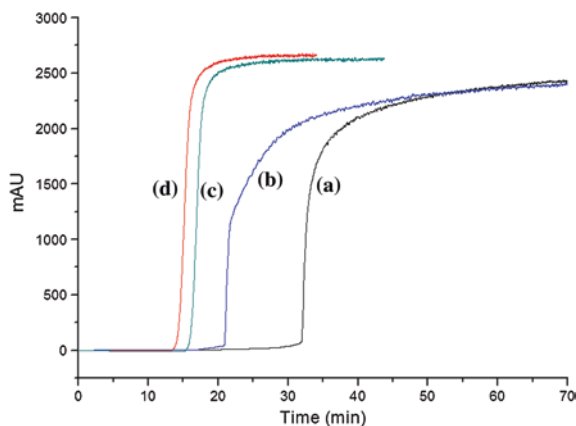


**Fig. 2.8** Dynamic adsorption curves of the synthetic peptide by frontal analysis with 7-cm-long phosphate monolithic column (a) and 2-cm-long packed polysulfoethyl A column (b). The void time was estimated by flushing 50 mM benzoic acid for packed SCX column (c) and phosphate monolithic column (d), the UV adsorption wavelength was set at 280 nm (Reprinted with permission from Ref. [38]. Copyright 2007 American Chemical Society)

which indicates faster kinetic adsorption of the peptide on the phosphate monolith than on the Polysulfoethyl A particles due to the porous structure of phosphate monolith. Further, the phosphate monolith specifically exhibits SCX mechanism because only one plateau was observed in the frontal analysis curve.

#### **2.2.4 Application of Phosphate SCX Monolithic Column in Automated Sample Injection and SCX-RP 2D LC-MS/MS Analyses**

The 150  $\mu\text{m}$  i.d.  $\times$  7 cm phosphate SCX monolithic column was used as trap column for fast sample injection followed with RP gradient LC separation by using 75  $\mu\text{m}$  i.d.  $\times$  12 cm C18 packed column (Fig. 2.9). First, tryptic digest of 1  $\mu\text{g}$  yeast protein extract was automatically loaded onto the SCX monolithic column at 2  $\mu\text{L}/\text{min}$ . Then, the analytes onto the SCX monolithic column were transferred to C18 separation column by 10 min elution with 1,000 mM  $\text{NH}_4\text{AC}$  (pH 2.7) as described in Experimental Section and nanoflow LC-MS/MS was performed (Fig. 2.10). It could be seen that the efficient LC separation time window was about 90 min, which was consistent with the time range from 10 to 35 % ACN. Therefore, little sample loss was occurred during the processes of sample injection. By examining the elution profile of a moderate intensity peptide of K.ATAGDTHLGGEDFDNR.L ( $m/z = 838$ , +2) extracted from the separation chromatograms, peak capacity of 359 could be calculated with  $\sim$ 90-min separation window. After database searching and controlling FDR < 1 %, with the spectra



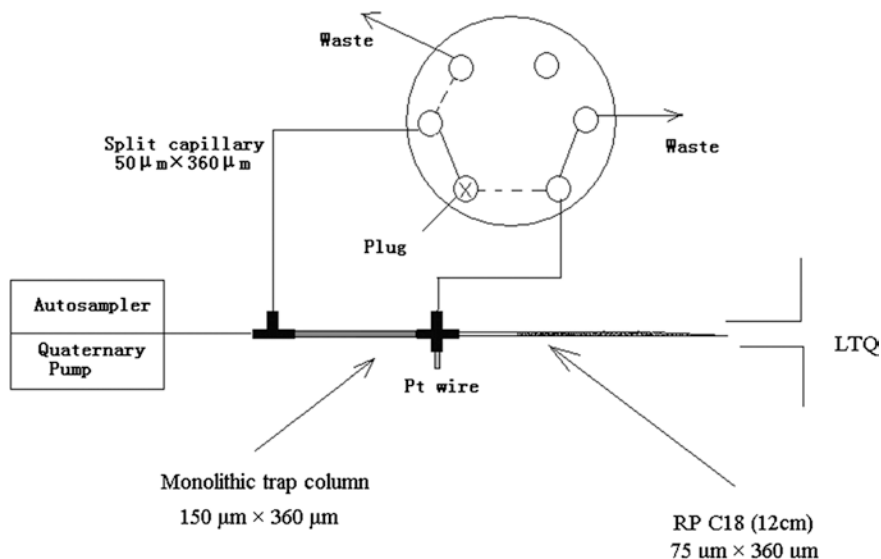


**Fig. 2.9** Schematic diagram of the SCX monolithic column online sample injection system. *Solid line* loading sample onto trap column; *dashed line* eluting sample to analytical column and gradient RPLC analysis (Reprinted with permission from Ref. [38]. Copyright 2007 American Chemical Society)

filtered with the above criteria, 1,578 unique peptides were positively identified from 460 distinct proteins of yeast proteome. These results were much better than that obtained by 2 cm packed SCX trap column as described in Sect. 2.2.2. Therefore, increasing the sample loading capacity of trap column is important to improve the performance of proteome analyses.

As the SCX monolithic column has more than 10 times higher permeability than packed SCX column, the sample loading flow rate ranged from 2 to 40 μL/min were invested (Fig. 2.11). Obviously, the flow rate of sample injection has little influence on the numbers of identified peptides and proteins even if the sample injection flow rate increases 20 times. Therefore, sample injection with ultra-high flow rate is feasible, which could improve the throughput of proteome analyses significantly. Then, six times replicate analyses were performed for 1 μg yeast protein and the LC retention time of 10 randomly selected peptides were investigated (Table 2.4). The RSDs for all the retention time of the 10 peptides were almost less than 1 %, which demonstrated the high reproducibility of the automated sample injection system using SCX monolithic trap column in LC separation. Further, 1,556 unique peptides (RSD = 2.0 %) corresponding to 452 distinct proteins (RSD = 0.7 %) were averagely identified from the six replicate analyses, which also demonstrated the good reproducibility of SCX monolithic column system in proteome analyses.

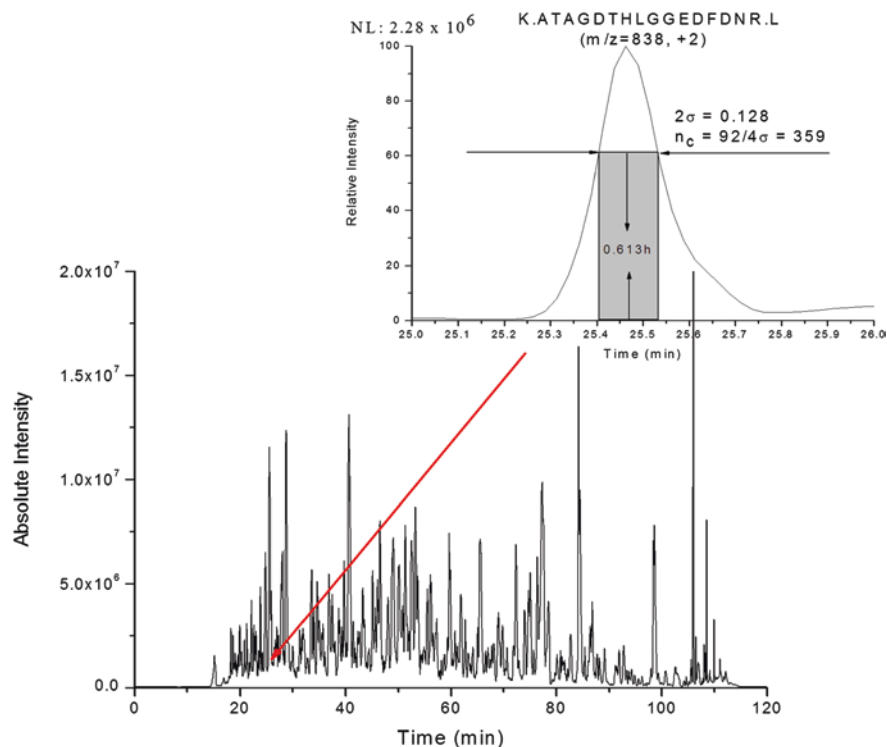


**Fig. 2.10** Base peak chromatograms for nano-RPLC-MS/MS analysis of 1  $\mu$ g yeast proteins tryptic digest on the automated sample injection system using phosphate monolithic trap column (Reprinted with permission from Ref. [38]. Copyright 2007 American Chemical Society)

One-dimensional RP LC separation is usually not enough for comprehensive proteome analysis of complex protein sample as described above. Therefore, SCX-RP 2D LC-MS/MS analysis was also performed for this SCX monolithic column system. After 20  $\mu$ g tryptic digest of yeast protein extract was automated loaded onto the SCX monolithic column, 17 cycles of salt steps were applied to fractionate the peptides mixture to the C18 separation column, and a nanoflow RP LC MS/MS analysis with 90 min binary RP separation gradient from 10 to 35 % ACN was performed after each fractionation as described in Experimental Section (Fig. 2.12). After database searching and controlling the FDR < 1 % ( $\Delta C_n = 0.39$ ), 5,608 unique peptides (totally 54,780 peptides) corresponding to 1,522 distinct protein groups were successfully characterized. Comparing to the one-dimensional RPLC separation, the proteome coverage was increased 230 %, which is also much better than the results obtained by 2-cm-long SCX packed trap column as described in Sect. 2.2.2. Therefore, the phosphate SCX monolithic column exhibited superior performance in automated sample injection and online 2D

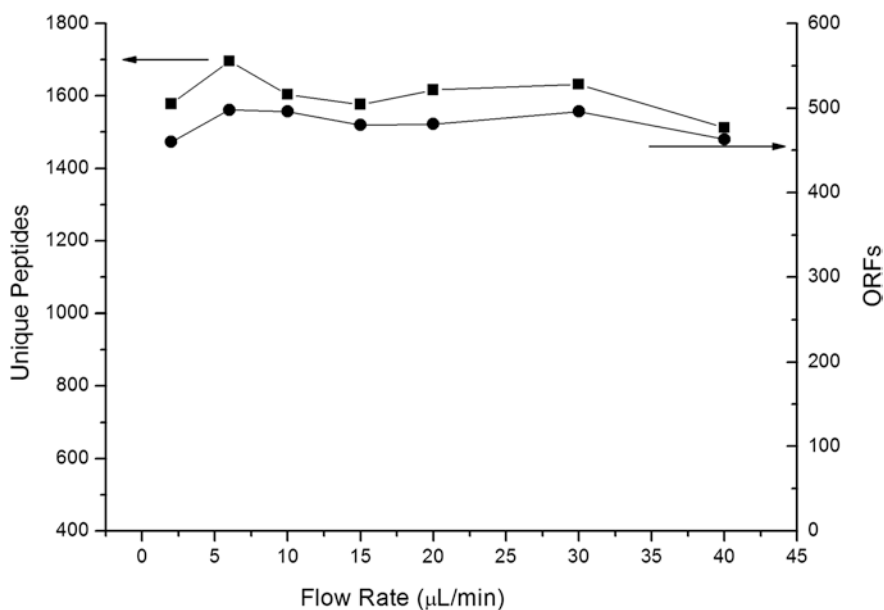


**Fig. 2.11** Effect of sample loading flow rate on the number of unique peptides and distinct proteins identified by the automated sample injection system using phosphate monolithic trap column (Reprinted with permission from Ref. [38]. Copyright 2007 American Chemical Society)

**Table 2.4** Run-to-run reproducibility of six consecutive nano-RPLC-MS/MS analyses for 1 μg yeast protein tryptic digest by using phosphate monolithic trap column with the automated sample injection\*

Mass	Retention time							RSD (%)
	Run 1	Run 2	Run 3	Run 4	Run 5	Run 6	Ave.	
1,017.57	17.84	18.40	18.28	18.41	18.53	18.60	18.34	1.4
883.52	29.20	29.72	29.38	29.22	29.59	29.46	29.43	0.6
1,416.72	35.75	36.29	36.38	36.10	36.42	36.44	36.23	0.7
925.61	43.06	43.70	43.85	43.54	43.87	44.01	43.67	0.7
1,752.79	48.32	49.00	49.01	48.71	49.26	49.18	48.91	0.6
1,351.75	56.22	56.92	56.70	56.67	56.88	56.99	56.73	0.4
2,259.23	68.55	69.19	69.17	68.92	69.00	69.02	68.97	0.3
2,388.20	76.51	76.57	76.69	76.30	76.66	76.66	76.56	0.2
2,831.45	83.39	83.56	83.65	83.59	83.76	83.70	83.61	0.1
1,821.92	88.40	89.35	89.08	89.13	89.36	89.32	89.11	0.4

Reprinted with permission from Ref. [38]. Copyright 2007 American Chemical Society

\*Peptides are randomly selected across the elution, and separation conditions are the same as for Fig. 2.10

SCX-RP nanoflow LC-MS/MS for proteome analysis. This can be attributed to its high sample loading capacity and pure SCX retention mechanism, which greatly improve the resolution of SCX fractionation in 2D LC separation.

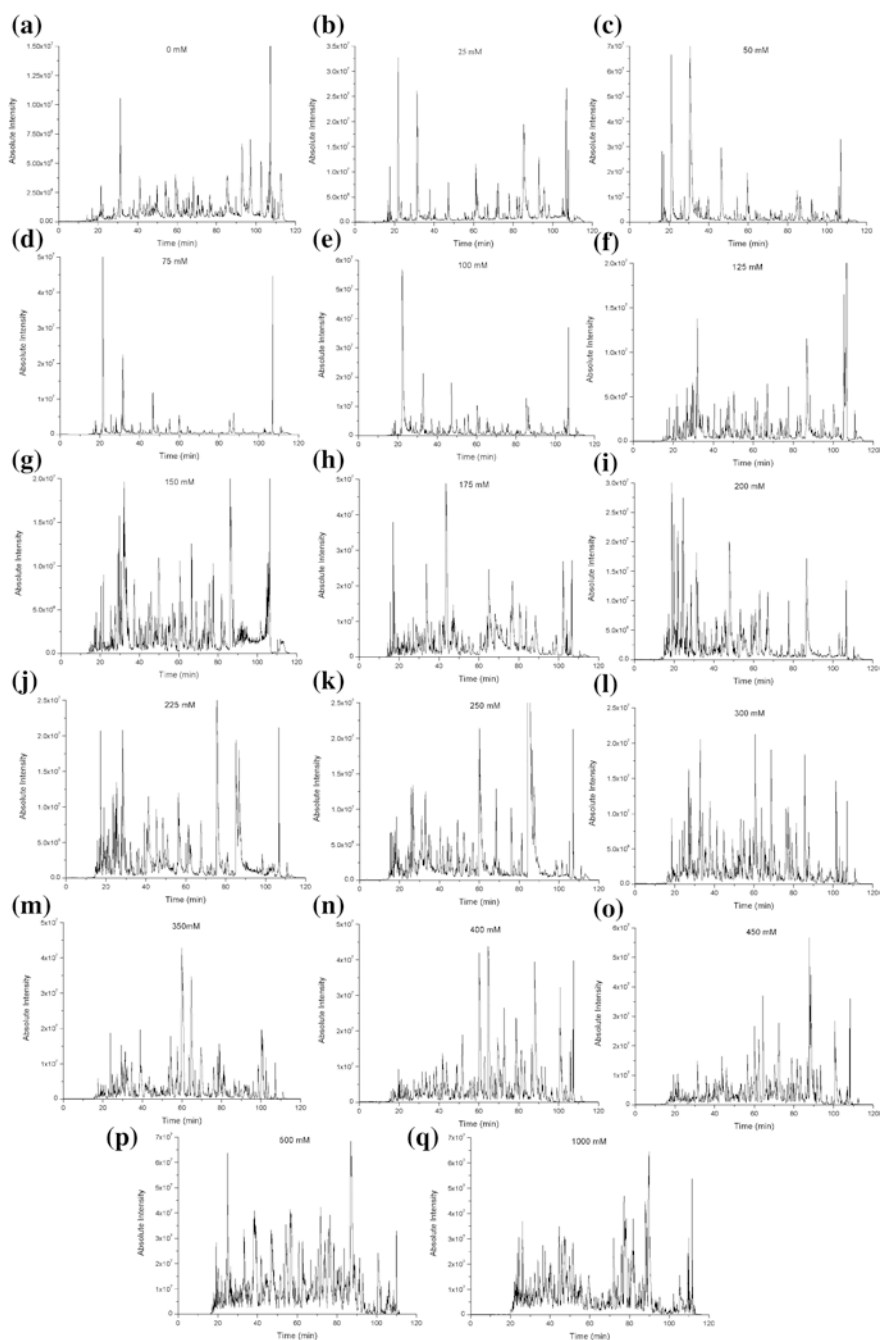


**Fig. 2.12** Chromatograms of a 17-cycle online multidimensional analysis of tryptic digest of 20  $\mu\text{g}$  yeast proteins (Reprinted with permission from Ref. [38]. Copyright 2007 American Chemical Society)

## 2.3 Conclusion

This chapter focuses on the automated sample injection and online multidimensional LC separation in proteome analyses. First, we systematically studied the influence of dead volume between trap and LC separation column on the performance of LC separation and proteome analyses for SCX, C18, and C8 trap column systems. The tolerance of trap column to dead volume is  $SCX \gg C8 > C18$ , and SCX trap column system also exhibited the best performance in proteome analyses. Therefore, SCX trap column is more suitable for automated sample injection in nanoflow LC-MS/MS system. Then, an automated sample-clean system was established by SCX trap column and 10-port nanoswitching valve, and superior performance was obtained for proteome analysis of uncleaned protein digest due to the low protein sample loss in online purification. Finally, a phosphate SCX monolithic column was prepared for automated sample injection and online fractionation of the peptides mixture. Comparing with packed SCX column, 10 times higher permeability was exhibited, and sample injection flow rate as high as 40  $\mu\text{L}/\text{min}$  could be realized. Furthermore, high sample loading capacity was also achieved for the SCX monolithic column, which significantly improved the resolution in online fractionation and also for the proteome coverage in SCX-RP 2D LC-MS/MS analyses.

## 2.4 Experimental Section

### 2.4.1 Materials

Daisogel ODS-AQ (5  $\mu\text{m}$ , 12 nm pore) was purchased from DAISO Chemical CO., Ltd. (Osaka, Japan), Magic C18AQ (5  $\mu\text{m}$ , 20 nm pore) was purchased from Michrom BioResources (Auburn, CA, USA), and Polysulfoethyl Aspartamide (5  $\mu\text{m}$ , 20 nm pore) was a gift from PolyLC Inc. (Columbia, MD, USA). PEEK tubing, sleeves, microtee, microcross, and mini microfilter assembly (with a filter capsule, porosity 2  $\mu\text{m}$ ) were obtained from Upchurch Scientific (Oak Harbor, WA, USA). Fused silica capillaries with 75 and 150  $\mu\text{m}$  i.d. were purchased from Polymicro Technologies (Phoenix, AZ, USA), and 50  $\mu\text{m}$  i.d. from Yongnian Optical Fiber Factory (Hebei, China). All the water used in experiments was purified using a Mill-Q system from Millipore Company (Bedford, MA, USA). Dithiothreitol (DTT), iodoacetamide were both purchased from Sino-American Biotechnology Corporation (Beijing, China). Ethylene glycol methacrylate phosphate (EGMP), bis-acrylamide, dimethylsulfoxide, dodecanol, N, N'-dimethylformamide, and  $\gamma$ -methacryloxypropyltrimethoxysilane ( $\gamma$ -MAPS) were obtained from Sigma (St. Louis, MO, USA). Azobisisobutyronitrile (AIBN) was obtained from Shanghai Fourth Reagent Plant (Shanghai, China). Trypsin was obtained from Promega (Madison, WI, USA). Synthetic peptide was purchased

from Serva (Heidelberg, Germany), and Tris was from Amersco (Solon, Ohio, USA). Formic acid was obtained from Fluka (Buches, Germany). Acetonitrile (ACN, HPLC grade) was from Merck (Darmstadt, Germany).

### ***2.4.2 Sample Preparation***

The yeast protein extract was prepared in a denaturing buffer containing 50 mM Tris/HCl (pH 8.1) and 8 M urea. The protein concentration was determined by BCA assay. The protein sample was reduced by DTT at 37 °C for 2 h and alkylated by iodoacetamide in dark at room temperature for 40 min. Then the solution was diluted to 1 M urea with 50 mM Tris/HCl (pH 8.1). Finally, trypsin was added with weight ratio of trypsin to protein at 1/25 and incubated at 37 °C overnight. Then, the tryptic digest was purified with a homemade C18 solid phase cartridge and exchanged into 0.1 % FA water solution. Finally, the samples were stored at −20 °C before usage.

### ***2.4.3 Preparation of Particles Packed Columns***

Particulate columns were packed using a homemade pneumatic pressure cell at constant nitrogen gas pressure of about 580 psi with a slurry packing method. For the preparation of C18 separation column, one end of a 75  $\mu\text{m}$ -i.d. fused silica capillary was manually pulled to a fine point of  $\sim 5\ \mu\text{m}$  with a flame torch at first, and then 12-cm-long C18 particles (5  $\mu\text{m}$ , 12 nm pore) were packed. After a mini microfilter assembly (with a filter capsule, porosity 2  $\mu\text{m}$ ) was placed on one end of a 150  $\mu\text{m}$ -i.d. capillary, 1- or 2-cm-long SCX or C18 material (5  $\mu\text{m}$ , 20 nm pore) was packed into the column to prepare the particulate SCX or C18 trap column. After the column was packed with appropriate length, it was connected to a LC pump and equilibrated with 0.1 % FA water solution at  $\sim 1,500$  psi for at least 30 min before usage. The 2-cm-long particulate SCX column was used to measure the dynamic binding capacity of Polysulfoethyl A and 1-cm-long particulate SCX and C18 trap columns were used in permeability measurement. 2-cm-long particulate trap columns were also used for sample injection in proteome analysis.

### ***2.4.4 Preparation of Phosphate Monolithic Capillary Column***

Prior to the polymerization, the capillary was pretreated with  $\gamma$ -MAPS [37]. The reaction mixture consisting of EGMP (80  $\mu\text{L}$ ,  $\sim 100$  mg), bis-acrylamide (60 mg), dimethylsulfoxide (270  $\mu\text{L}$ ), dodecanol (200  $\mu\text{L}$ ), N, N'-dimethylformamide (50  $\mu\text{L}$ ), and AIBN (2 mg) was sonicated for 20 min to obtain a homogeneous

solution and then purged with nitrogen for 10 min. After the pretreated capillary was completely filled with the mixture, it was sealed at both ends with rubber stoppers. The sealed capillary was submerged into a water bath and allowed to react for 12 h at 60 °C. The resultant monolithic capillary column was washed with methanol for 2 h using an HPLC pump to remove unreacted monomers and porogens. Then, this phosphate monolithic capillary column could be directly used as the SCX trap column for proteome analysis without any other pretreatments.

Scanning electron microscopy (SEM) images of the monolithic column were obtained using a JEOL JSM-5,600 scanning electron microscope (JEOL Company, Japan).

#### ***2.4.5 Binding Capacity Measurement of the Phosphate Monolithic Capillary Column***

For measurement of the dynamic binding capacity, a synthetic peptide Leu-Trp-Met-Arg-Phe-NH<sub>2</sub>.HCOOH (Mw: 798.42) was used to saturate the phosphate monolithic column (150  $\mu$ m i.d., 7 cm) by frontal analysis. Briefly, 10 mg synthetic peptide was dissolved into 20 mL buffer containing 0.1 % FA and 10 % acetonitrile (pH 2–3), which was pumped through the phosphate monolith column at a constant flow rate of 20  $\mu$ L/min by a LC-10ADvp pump (Shimadzu). The solution from the monolithic column flowed into a 500 nL 1,100-DAD micro cell UV detector (Agilent). A 50-mM benzoic acid water solution containing 0.1 % FA and 10 % acetonitrile was used to estimate the void time of this system at the same flow rate because benzoic acid with considerable UV absorption is neutral in acidic solution.

To provide comparable data, the dynamic binding capacity of a particulate SCX column with 150  $\mu$ m i.d.  $\times$  2 cm was also measured following the same procedures.

#### ***2.4.6 Sample Injection***

The configuration for offline sample injection system by using C18, C8, or SCX trap columns was shown in Fig. 2.1. This system was used to systematically study the influence of dead volume between trap and analytical columns on the separation performance and proteomic coverage. During sample loading, the 6-port/two-position valve was switched to close the split flow, and 1  $\mu$ g SPE cleaned yeast protein digest (20  $\mu$ L) was injected by Surveyor autosampler using the no-waste injection mode at a flow rate of 2  $\mu$ L/min as shown in Fig. 2.1a. The mobile phase used was 0.1 % formic acid. After sample injection, the trap column and C18 separation column were manually connected by a ZDV (zero dead volume) union. Then the valve was switched to start the split flow in the front of



trap column. In order to investigate the influence of void volume on separation, appropriate void volume was introduced between trap and separation columns by using 150- $\mu\text{m}$ -i.d. void capillary as shown in Fig. 2.1b. And 5.7-, 16.9-, and 28.3-cm-long 150- $\mu\text{m}$ -i.d. void capillary were used to generate 1, 3, and 5  $\mu\text{L}$  dead volume, respectively.

The configuration for automated online sample injection of uncleaned protein sample using SCX or C18 trap column was shown in Fig. 2.5. The trap column was connected to a C18 separation column by a nanoflow switching valve and a microtee. During sample injection, the switching valve was switched to close the splitting flow and the flow through from the trap column was directed to waste. Yeast protein tryptic digest without SPE pretreatment (20  $\mu\text{L}$ ) was directly injected (Fig. 2.5 solid line mode) including 10 min for sample loading and 20 min for equilibration. After sample loading, the switching valve was switched to activate the splitting flow in the front of trap column and the flow through trap column was switched to the separation column at a rate  $\sim 200$  nL/min (Fig. 2.5 dashed line mode).

For manual injection, an open capillary filled with sample was connected between the microcross and the analytical column [39]. The peptides in the open capillary was flushed onto the analytical column by the 0.1 % FA at a flow rate of  $\sim 200$  nL/min (after splitting) and retained on the analytical column front. After sample loading, the open capillary was removed, and the separation column was directly connected to the microcross.

The configuration for automated sample injection using phosphate monolithic trap column was shown in Fig 2.9. During sample injection, the switching valve was switched to close the splitting flow and the flow through from the trap column was switched to waste (solid line mode in Fig. 2.9). We adjusted the time of sample injection at different flow rates to ensure the volume that flow though the trap column was three sample volumes for system equilibrium and removing contaminants. The sample solutions were loaded at flow rate of 2, 6, 10, 15, 20, 30, 40  $\mu\text{L}/\text{min}$  by setting loading times at 30, 10, 6, 4, 3, 2, 1.5 min, respectively, when 20  $\mu\text{L}$  sample was injected. After sample loading, the valve was switched to the dashed line mode and the gradient separation was automatically started.

#### 2.4.7 One-Dimensional LC Separation

The three buffer solutions used for the quaternary pump were 0.1 % FA water solution (buffer A), ACN with 0.1 % FA (buffer B), 1,000 mM  $\text{NH}_4\text{Ac}$  at pH 3 (buffer C). The flow rate after splitting was adjusted to separation optimal  $\sim 180$  nL/min. The binary gradient with buffer A and buffer B for RP separation was developed from 0 to 10 % buffer B for 2 min, from 10 to 35 % for 90 min, and from 35 to 80 % for 5 min. After flushing 80 % buffer B for 10 min, the separation system was equilibrated by buffer A for 13 min. In one-dimensional separation, the peptides retained on trap column were all eluted onto separation column by flushing with buffer C (containing 1,000 mM  $\text{NH}_4\text{Ac}$  at pH 3) for 10 min. After

the system was re-equilibrated with buffer A for 10 min, the binary separation gradient described above was started.

### ***2.4.8 Multidimensional LC Separation***

20  $\mu$ g tryptic digest of yeast protein was loaded automatically onto the particulate or monolithic SCX trap column. Then, a series of stepwise elution with salt concentrations of 0, 25, 50, 75, 100, 125, 150, 175, 200, 225, 250, 300, 350, 400, 450, 500, and 1000 mM  $\text{NH}_4\text{Ac}$  was used to gradually elute peptides from phosphate monolithic column onto the C18 analytical column (for particulate SCX trap column, 75, 125, 175, and 225 mM were not performed). Each salt step lasts 5 min except last one for 10 min. After whole system was re-equilibrated for 10 min with buffer A, the binary gradient elution described in Sect. 2.4.7 was applied to separate peptides prior to MS detection in each cycle.

### ***2.4.9 Mass Spectrometric Analysis***

The temperature of the ion transfer capillary was set at 200 °C. The spray voltage was set at 1.82 kV and the normalized collision energy was set at 35.0 %. One microscan was set for each MS and MS/MS scan. All MS and MS/MS spectra were acquired in the data-dependent mode. The mass spectrometer was set that one full MS scan was followed by six MS/MS scans on the six most intense ions. The dynamic exclusion function was set as follows: repeat count two, repeat duration 30 s, and exclusion duration 90 s. System control and data collection were done by Xcalibur software version 1.4 (Thermo).

### ***2.4.10 Data Analysis***

The acquired MS/MS spectra were searched on the database using the Turbo SEQUEST in the BioWorks 3.2 software suite (Thermo). The yeast database was downloaded from a website ([ftp://genome-ftp.stanford.edu/yeast/data\\_download/sequence/genomic\\_sequence/orf\\_protein/orf\\_trans.fasta.gz](ftp://genome-ftp.stanford.edu/yeast/data_download/sequence/genomic_sequence/orf_protein/orf_trans.fasta.gz)). Reversed sequences were appended to the database for the evaluation of false positive rate. Cysteine residues were searched as static modification of 57.0215 Da, and methionine residues as variable modification of +15.9949 Da. Peptides were searched using fully tryptic cleavage constraints and up to two internal cleavages sites were allowed for tryptic digestion. The mass tolerances were 2 Da for parent masses and 1 Da for fragment masses. The peptides were considered as positive identification if

the Xcorr were higher than 1.9 for singly charged peptide, 2.2 for doubly charged peptide, and 3.75 for triply charged peptides.  $\Delta C_n$  cutoff value was set to control the false positive rate of peptides identification  $<1\%$ , determined by the calculation based on the reversed database 12.

## References

1. Link AJ, Eng J, Schieltz DM, Carmack E, Mize GJ, Morris DR, Garvik BM, Yates JR (1999) Direct analysis of protein complexes using mass spectrometry. *Nat Biotechnol* 17:676–682
2. Wolters DA, Washburn MP, Yates JR (2001) An automated multidimensional protein identification technology for shotgun proteomics. *Anal Chem* 73:5683–5690
3. Jiang X, Feng S, Tian R, Han G, Ye M, Zou H (2007) Automation of nanoflow liquid chromatography-tandem mass spectrometry for proteome analysis by using a strong cation exchange trap column. *Proteomics* 7:528–539
4. Ishihama Y (2005) Proteomic LC-MS systems using nanoscale liquid chromatography with tandem mass spectrometry. *J Chromatogr A* 1067:73–83
5. van der Heeft E, ten Hove GJ, Herberts CA, Meiring HD, van Els CA, de Jong AP (1998) A microcapillary column switching HPLC-electrospray ionization MS system for the direct identification of peptides presented by major histocompatibility complex class I molecules. *Anal Chem* 70:3742–3751
6. Shen Y, Tolić N, Masselon C, Paša-Tolić L, Camp DG, Hixson KK, Zhao R, Anderson GA, Smith RD (2003) Ultrasensitive proteomics using high-efficiency on-line micro-SPE-nanoLC-nanoESI MS and MS/MS. *Anal Chem* 76:144–154
7. Shen Y, Zhang R, Moore RJ, Kim J, Metz TO, Hixson KK, Zhao R, Livesay EA, Udseth HR, Smith RD (2005) Automated 20 kpsi RPLC-MS and MS/MS with chromatographic peak capacities of 1000–1500 and capabilities in proteomics and metabolomics. *Anal Chem* 77:3090–3100
8. Licklider LJ, Thoreen CC, Peng J, Gygi SP (2002) Automation of nanoscale microcapillary liquid chromatography-tandem mass spectrometry with a vented column. *Anal Chem* 74:3076–3083
9. Meiring HD, Van Der Heeft E, Ten Hove GJ, De Jong APJM (2002) Nanoscale LC-MS: technical design and applications to peptide and protein analysis. *J Sep Sci* 25:557–568
10. Yi EC, Lee H, Aebersold R, Goodlett DR (2003) A microcapillary trap cartridge-microcapillary high-performance liquid chromatography electrospray ionization emitter device capable of peptide tandem mass spectrometry at the attomole level on an ion trap mass spectrometer with automated routine operation. *Rapid Commun Mass Spectrom* 17:2093–2098
11. Kang D, Nam H, Kim YS, Moon MH (2005) Dual-purpose sample trap for on-line strong cation-exchange chromatography/reversed-phase liquid chromatography/tandem mass spectrometry for shotgun proteomics: application to the human jurkat T-cell proteome. *J Chromatogr A* 1070:193–200
12. Wu L, Han DK (2006) Overcoming the dynamic range problem in mass spectrometry-based shotgun proteomics. *Expert Rev Proteomics* 3:611–619
13. Shen Y, Moore RJ, Zhao R, Blonder J, Auberry DL, Masselon C, Paša-Tolić L, Hixson KK, Auberry KJ, Smith RD (2003) High-efficiency on-line solid-phase extraction coupling to 15–150  $\mu\text{m}$ -i.d. Column liquid chromatography for proteomic analysis. *Anal Chem* 75:3596–3605
14. Shen Y, Zhao R, Berger SJ, Anderson GA, Rodriguez N, Smith RD (2002) High-efficiency nanoscale liquid chromatography coupled on-line with mass spectrometry using nanoelectrospray ionization for proteomics. *Anal Chem* 74:4235–4249

15. Vollmer M, Hörth P, Nägele E (2004) Optimization of two-dimensional off-line LC/MS separations to improve resolution of complex proteomic samples. *Anal Chem* 76:5180–5185
16. Peng J, Elias JE, Thoreen CC, Licklider LJ, Gygi SP (2003) Evaluation of multidimensional chromatography coupled with tandem mass spectrometry (LC/LC-MS/MS) for large-scale protein analysis: the yeast proteome. *J Proteome Res* 2:43–50
17. Wagner K, Miliotis T, Marko-Varga G, Bischoff R, Unger KK (2002) An automated on-line multidimensional HPLC system for protein and peptide mapping with integrated sample preparation. *Anal Chem* 74:809–820
18. Xiang R, Shi Y, Dillon DA, Negin B, Horváth C, Wilkins JA (2004) 2D LC/MS analysis of membrane proteins from breast cancer cell lines MCF7 and BT474. *J Proteome Res* 3:1278–1283
19. Opiteck GJ, Jorgenson JW, Anderegg RJ (1997) Two-dimensional SEC/RPLC coupled to mass spectrometry for the analysis of peptides. *Anal Chem* 69:2283–2291
20. Lohaus C, Nolte A, Blüggel M, Scheer C, Klose J, Gobom J, Schüler A, Wiebringhaus T, Meyer HE, Marcus K (2006) Multidimensional chromatography: a powerful tool for the analysis of membrane proteins in mouse brain. *J Proteome Res* 6:105–113
21. Gilar M, Daly AE, Kele M, Neue UD, Gebler JC (2004) Implications of column peak capacity on the separation of complex peptide mixtures in single- and two-dimensional high-performance liquid chromatography. *J Chromatogr A* 1061:183–192
22. Washburn MP, Wolters D, Yates JR (2001) Large-scale analysis of the yeast proteome by multidimensional protein identification technology. *Nat Biotechnol* 19:242–247
23. Zou H, Huang X, Ye M, Luo Q (2002) Monolithic stationary phases for liquid chromatography and capillary electrochromatography. *J Chromatogr A* 954:5–32
24. Svec F (2004) Preparation and HPLC applications of rigid macroporous organic polymer monoliths. *J Sep Sci* 27:747–766
25. Svec F (2004) Organic polymer monoliths as stationary phases for capillary HPLC. *J Sep Sci* 27:1419–1430
26. Xie C, Ye M, Jiang X, Jin W, Zou H (2006) Octadecylated silica monolith capillary column with integrated nanoelectrospray ionization emitter for highly efficient proteome analysis. *Mol Cell Proteomics* 5:454–461
27. Wu R, Zou H, Ye M, Lei Z, Ni J (2001) Separation of basic, acidic and neutral compounds by capillary electrochromatography using uncharged monolithic capillary columns modified with anionic and cationic surfactants. *Electrophoresis* 22:544–551
28. Liu Z, Wu R, Zou H (2002) Recent progress in adsorbed stationary phases for capillary electrochromatography. *Electrophoresis* 23:3954–3972
29. Viklund C, Svec F, Frechet JM, Irgum K (1997) Fast ion-exchange HPLC of proteins using porous poly(glycidyl methacrylate-co-ethylene dimethacrylate) monoliths grafted with poly(2-acrylamido-2-methyl-1-propanesulfonic acid). *Biotechnol Prog* 13:597–600
30. Ueki Y, Umemura T, Li J, Odake T, Tsunoda K (2004) Preparation and application of methacrylate-based cation-exchange monolithic columns for capillary ion chromatography. *Anal Chem* 76:7007–7012
31. Peters EC, Petro M, Svec F, Fréchet JMJ (1997) Molded rigid polymer monoliths as separation media for capillary electrochromatography. *Anal Chem* 69:3646–3649
32. Peters EC, Petro M, Svec F, Fréchet JMJ (1998) Molded rigid polymer monoliths as separation media for capillary electrochromatography. 1. Fine control of porous properties and surface chemistry. *Anal Chem* 70:2288–2295
33. Wu R, Zou H, Fu H, Jin W, Ye M (2002) Separation of peptides on mixed mode of reversed-phase and ion-exchange capillary electrochromatography with a monolithic column. *Electrophoresis* 23:1239–1245
34. Gu B, Chen Z, Thulin CD, Lee ML (2006) Efficient polymer monolith for strong cation-exchange capillary liquid chromatography of peptides. *Anal Chem* 78:3509–3518

35. Wang F, Jiang X, Feng S, Tian R, Han G, Liu H, Ye M, Zou H (2007) Automated injection of uncleaned samples using a ten-port switching valve and a strong cation-exchange trap column for proteome analysis. *J Chromatogr A* 1171:56–62
36. Fu H, Xie C, Dong J, Huang X, Zou H (2004) Monolithic column with zwitterionic stationary phase for capillary electrochromatography. *Anal Chem* 76:4866–4874
37. Dong J, Zhou H, Wu R, Ye M, Zou H (2007) Specific capture of phosphopeptides by  $Zr^{4+}$ -modified monolithic capillary column. *J Sep Sci* 30:2917–2923
38. Wang F, Dong J, Jiang X, Ye M, Zou H (2007) Capillary trap column with strong cation-exchange monolith for automated shotgun proteome analysis. *Anal Chem* 79:6599–6606
39. Feng S, Ye M, Jiang X, Jin W, Zou H (2006) Coupling the immobilized trypsin microreactor of monolithic capillary with  $\mu$ RPLC–MS/MS for shotgun proteome analysis. *J Proteome Res* 5:422–428

Applications of Monolithic Column and Isotope  
Dimethylation Labeling in Shotgun Proteome Analysis

Wang, F.

2014, XIII, 94 p. 42 illus., 23 illus. in color., Hardcover

ISBN: 978-3-642-42007-8